# Theoretical studies of the angular distributions of oxygen atoms ejected from an ion bombarded $c(2\times2)$ overlayer of oxygen on Ni(001). I. Effect of geometry

Shukla Kapur[a] and Barbara J. Garrison[b]

*Department of Chemistry, The Pennsylvania State University, University Park, Pennsylvania 16802*
(Received 20 January; accepted 10 March 1981)

A detailed molecular dynamics study has been performed in order to determine the factors controlling the ejection directions of adsorbate atoms due to 600 eV $Ar^+$ ion bombardment. The specific system studied is oxygen which dissociatively adsorbs to form a $c(2\times2)$ overlayer on Ni(001). A fourfold bridge, an atop or linear and twofold bridge bond, as well as several heights of the oxygen atoms above the surface were investigated. The angular distributions are shown to be influenced by both the bonding site and the height of the oxygen adsorbate. There are distinguishing characteristics that can be ascribed to each of these three bonding sites.

## I. INTRODUCTION

Considerable effort has been expended in the past decade in developing techniques that can measure the geometry of atoms and small molecules adsorbed on surfaces. These techniques include low energy electron diffraction (LEED),[1] electron stimulated desorption ion angular distributions (ESDIAD),[2] energy loss spectroscopy (ELS),[3] ion scattering (ISS, LEIS, MEIS, HEIS),[4] surface extended x-ray absorption fine structure (SEXAFS),[5] and angle-resolved secondary ion mass spectrometry (SIMS).[6] Of particular interest here is the proposal that the angular distributions of particles ejected during keV ion bombardment of a solid are sensitive to both the original site of an adsorbed atom and to its height above the surface.[6,7] Preliminary experiments have shown highly anisotropic distributions for the ejected species $Cu^+$,[6] $O^-$,[6] $Ni^+$,[8] $Ni_2^+$,[8] $Ni_3^+$,[8] $S^-$,[9] and $NiCO^+$.[10]

Since angle-resolved SIMS measurements are in their initial stages, theoretical studies are required to determine the sensitivity of the angular distributions to differing original geometries of the adsorbate. This is a necessary first step in ascertaining how accurately bond lengths and bonding sites of adsorbates on surfaces can be measured. The theoretical approach we have chosen is the classical dynamics model that led to the prediction that the angular distributions of ejected particles would be sensitive to their original sites on the surface.[7] As a model system, we have chosen oxygen which adsorbs dissociatively and forms a $c(2\times2)$ overlayer on Ni(001). LEED calculations have shown the oxygen to be situated 0.9 Å above the surface plane.[11]

We will be focusing on only the high energy ($\geq$10 eV) oxygen atoms which eject, since these appear to contain the most structural information.[7] These high energy particles generally leave early in the collision cascade while the surface is still highly ordered and can control their angle of ejection. The low energy particles, on the other hand, tend to leave late in the cascade, when the surface is damaged, and, as a consequence, their angular distribution is more isotropic. Another reason for only analyzing the high energy particles is that the theoretical model predicts the angular distributions of all particles (mainly neutrals) that are ejected while SIMS experiments detect only ejected ions. The image force, which acts perpendicularly to the surface, may influence the polar angle by a few degrees but should not affect the azimuthal angle. Some preliminary evidence for this effect has recently been found for the CO on Ni(001) system.[12] The influence of the image force on ejecting ions will be much smaller for the faster moving particles. It should also be noted that for clean copper exposed to 5 keV $Ne^+$ ion bombardment under high dose conditions, the angular distributions of the copper ions and neutrals have been found to be similar.[13]

There are two aspects to be explored before one can use the angular distributions of the ejected particles to determine geometries. First, assuming that we know the forces among the atoms, how sensitive are the ejection angles to changes in bonding sites and lengths? Second, since we do not accurately know these interactions, how sensitive are the angular distributions to changes in the potential energies or forces? This study will concentrate on the first part of this problem, that of the sensitivity of the angular distributions to geometry. A subsequent paper[14] will examine the influence of changes in the interaction potential on our ability to compute angular distributions associated with specific adsorbate locations.

## II. DESCRIPTION OF THE CALCULATION

The basic scheme for computing the dynamics of the bombarding ion, the metal substrate, and the adsorbates has been described in a recent series of articles.[15–18] Briefly, the positions and momenta of all the particles are developed in time by integrating Hamilton's equations of motion. The final positions and momenta of the ejected particles can then be used to determine yields, energy and angular distributions, and possible cluster formation.

The specific system to be studied here is atomic

[a]Present address: Department of Physics, Rochester Institute of Technology, Rochester, N. Y. 14623.
[b]Alfred P. Sloan Research Fellow.

 0021-9606/81/130445-08$01.00  

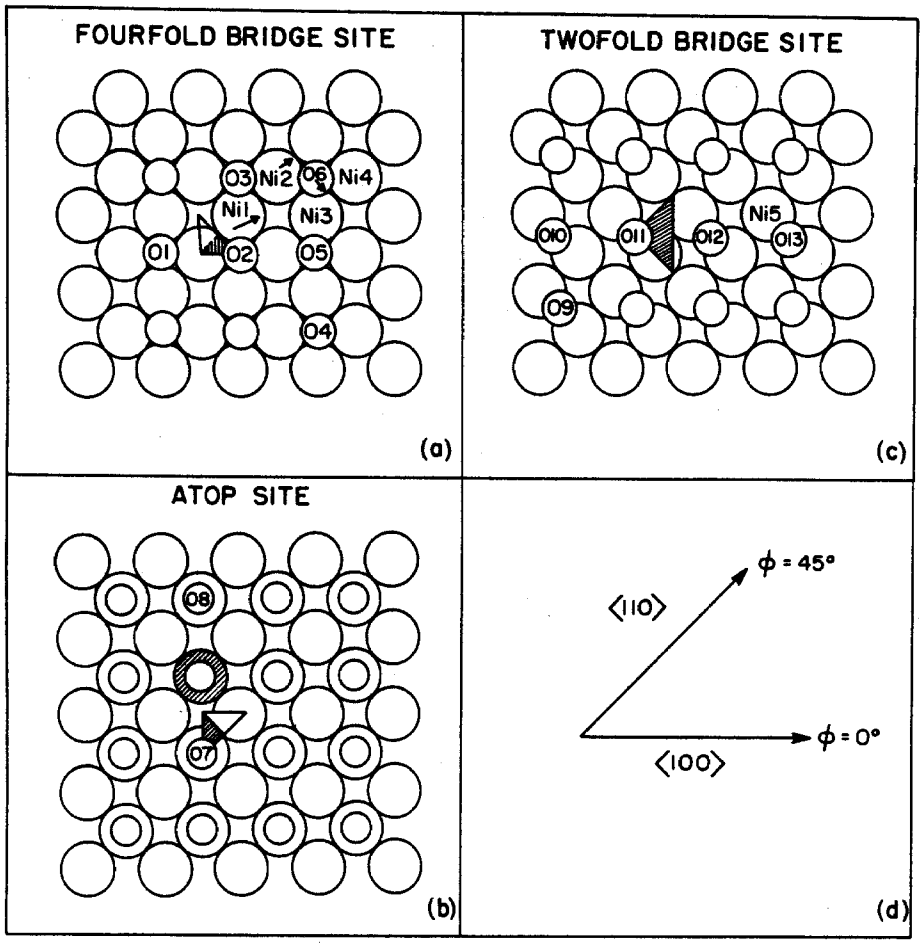


FIG. 1. Ni(001) with oxygen adsorbates. The larger circles represent nickel atoms while the smaller ones represent oxygen atoms. For each adsorption site, the size of the surface and placement of adsorbates are shown. The large triangle is the impact zone of irreducible symmetry with the shaded part giving rise to the ejection of high energy oxygen atoms. The numbers are labels used in the text. The arrows denote the direction of motion of the atoms (see the text): (a) fourfold bridge bonded site; (b) atop or linear bonded site; (c) twofold bridge bonded site; (d) crystal directions.

oxygen which adsorbs in a $c(2\times2)$ overlayer on Ni(001). Although experimentally the oxygen is believed to bond in a fourfold bridge site 0.9 Å above the surface plane,[11] theoretically we can place it in any position. We have chosen to examine three high symmetry sites: a fourfold bridge bond, an atop or linear bond, and a twofold bridge bond. In addition, we vary the height of the oxygen atom above the surface for each of these sites. The placement of the oxygen atoms on the Ni(001) surface for each of these sites is shown in Fig. 1. The primary ion used for the bombardment is $Ar^+$ with 600 eV of energy at normal incidence. Also shown in Fig. 1 is the impact zone of irreducible symmetry in which the $Ar^+$ ion must bombard so as to be comparable with experimental observables.

The infinite solid is replaced by a finite microcrystallite in the calculations. In other studies where *all* experimental observables were of interest, a crystallite of four layers with ~60 atoms/layer was used.[15] If adsorbates are included, this results in 250–300 atoms which are followed explicitly in the dynamics calculations. Typically, it is necessary to calculate 50–200 ion impacts to compare averaged quantities with experimental results. Each ion impact is quite lengthy, taking ~30–60 sec on an IBM 370 model 3033. This time is approximately proportional to the square of the number of atoms in the crystallite.

Since for this study there are many geometries for which calculations needed to be performed, we started looking for ways to reduce the computational effort. Since only the angular distributions of the ejected oxygen atoms with greater than 10 eV of kinetic energy are of interest, these distributions were examined as a function of the number of atoms in the crystallite. Using a sample of only two layers with ~35 Ni atoms/layer gave the same angular distributions as the large 250 atom crystallite, but with considerably reduced computer time. Physically, this reduction in crystallite size is valid because the high energy particles leave early in the collision cascade and generally originate from near the $Ar^+$ ion impact point. In contrast, low energy processes generally occur late in the cascade and are much more dependent on the atoms in the lower layers and on the edges of the crystallite. In addition, we found that $Ar^+$ ion impacts in only part of the impact zone caused motion such that high energy oxygen atoms ejected. Thus, two modifications of the previous method have been made. First, a crystallite of two Ni layers with ~35–40 Ni atoms/layer and with 9–16 adsorbed oxygen atoms is used (see Fig. 1 for arrangements of top layer and of oxygen atoms). Second, only ion impacts in the active part of the zone shown in Fig. 1 were calculated. The effect of these modifications have only been tested for the angular distributions of ejected oxygen atoms with greater than 10 eV of energy. To use this small crystal to calculate other specific variables or systems would require retesting.

TABLE I. Potential parameters.

| | $A$ (keV) | $B$ (Å$^{-1}$) | $D_e$ (eV) | $\beta$ (Å$^{-1}$) | $R_e$ (Å) | $R_a$ (Å) | $R_b$ (Å) | $R_c$ (Å) |
|---|---|---|---|---|---|---|---|---|
| Ar–Ni | 68.844 | 4.593 | 0.0 | 0.0 | 0.0 | 2.49 | ... | ... |
| Ni–Ni | 21.035 | 5.088 | 0.58 | 1.47 | 2.55 | 1.46 | 1.94 | 4.22 |
| Ar–O | 19.67 | 4.593 | 0.0 | 0.0 | 0.0 | 2.49 | ... | ... |
| O–O | 1.72 | 5.088 | 0.48 | 1.405 | 2.628 | 1.76 | 2.24 | 3.43 |
| Ni–O | | | | | | | | |
| Fourfold bridge site | | | | | | | | |
| $z=0.9$ Å | ... | ... | 0.18 | 2.45 | 1.97 | ... | ... | 4.22 |
| Atop site | | | | | | | | |
| $z=2.0$ Å | ... | ... | 0.53 | 2.45 | 2.00 | ... | ... | 4.22 |
| Twofold bridge site | | | | | | | | |
| $z=1.56$ Å | ... | ... | 0.31 | 2.45 | 2.00 | ... | ... | 4.22 |

The most extensive height variations, 0.0 to 1.2 Å in steps of 0.1 Å, were performed for the oxygen in the fourfold bridge site. For the atop site, heights of 1.8, 2.0, 2.2, and 2.4 Å and, for the twofold bridge site, heights of 1.3, 1.56, 1.8, and 2.0 Å were examined. These were chosen assuming that an Ni–O separation distance of 2.0 Å from the LEED structure[11] is physically reasonable. This corresponds to heights of 0.9, 2.0, and 1.56 Å in the fourfold bridge, atop, and twofold bridge sites, respectively.

Since we are only examining the effect of the geometry on angular distributions and not the effect of the interaction potential, the potentials were chosen to be the same as those used previously.[16,18] We assume the total interaction to be pairwise additive. The general form of the pair potential for atoms in the bulk phase is composed of three parts: a repulsive Born–Mayer function for small internuclear separations, an attractive Morse potential at long range, and a cubic spline to connect the two. The composite pair potential $V$ between the two atoms separated by a distance $R$ is given by

$$V = A\,e^{-BR}, \quad R < R_a \,, \tag{1}$$

$$V = C_0 + C_1 R + C_2 R^2 + C_3 R^3, \quad R_a \le R \le R_b \,, \tag{2}$$

$$V = D_e\, e^{-\beta(R-R_e)}\,(e^{-\beta(R-R_e)} - 2.), \quad R_b < R < R_c \,, \tag{3}$$

$$V = 0, \quad R \ge R_c \,. \tag{4}$$

The interaction of $Ar^+$ with the other species is represented by a purely repulsive Born–Mayer function

$$V = A\,e^{-BR}, \quad R \le R_a \,, \tag{5}$$

$$V = 0, \quad R > R_a \,. \tag{6}$$

The parameters for the Ni–Ni, $Ar^+$–Ni, and $Ar^+$–O are the same as those used recently for a similar study with carbon monoxide adsorbed on Ni(001).[18] Briefly, these parameters are scaled to those developed over the last 15 years for Cu–Cu and $Ar^+$–Cu interactions.[19] Those values have been used to determine a wide range of experimental observables on Cu and should provide a comparative base for similar calculations on Ni. Thus, to alter the $A$ value in Eq. (1) or (5), we have chosen the screened Bohr form of the potential which adjusts $A$ by scaling to the products of the atomic numbers of the two atoms. The $B$ parameter has not been altered. We have scaled the Morse potential for $Cu_2$ to $Ni_2$ by using the $D_e$, $\beta$, and $R_e$ values reported by Girafalco and Weizer for $Ni_2$ and $Cu_2$.[20] The spline coefficients $C_i$ are determined so that the potential and its first derivative are continuous at $R_a$ and $R_b$.

Very little is known regarding the Ni–O pair potential. For simplicity we have chosen to use a Morse potential [Eq. (3)] for all internuclear separations. The value of $R_e$ that we use is determined by the distance between the oxygen atom and its nearest neighbor Ni atoms for a particular geometry. We have adjusted $D_e$ to keep the binding energy at 0.75 eV consistent with our earlier studies.[16] The Morse parameter $\beta$ is held constant at 2.45 Å$^{-1}$. The oxygen–oxygen pair potential is the same as used previously.[16] Examination of the important trajectories that result in high energy oxygen atoms ejecting shows that oxygen–oxygen interactions are virtually nonexistent except for the twofold bridge case. The potential parameters for selected geometries are given in Table I.

Using these potentials, approximately 100 ion impacts within the active part of the irreducible symmetry zone were calculated for each geometrical configuration. The kinetic energy $E$, polar angle $\theta$ as measured from the surface normal, and azimuthal angle $\phi$ of the ejected oxygen atoms were determined from the components of the final momentum. The ⟨100⟩ directions of the crystal correspond to $\phi = 0°$, 90°, 180°, ..., while the ⟨110⟩ directions correspond to $\phi = 45°$, 135°, 225°, ... (Fig. 1). It is the angular distributions of ejected oxygen atoms with $E \ge 10$ eV that are of interest here and will be discussed in the following section.

## III. RESULTS AND DISCUSSION

The sensitivity of the angular distributions of the ejected oxygen atoms to both site symmetry and adsorbate height will be discussed in this section. Each site will be considered individually. Following the analyses of the three sites will be a discussion of possible ways of comparing the theoretical results to experimental data.

The angular distribution of the ejected oxygen atoms

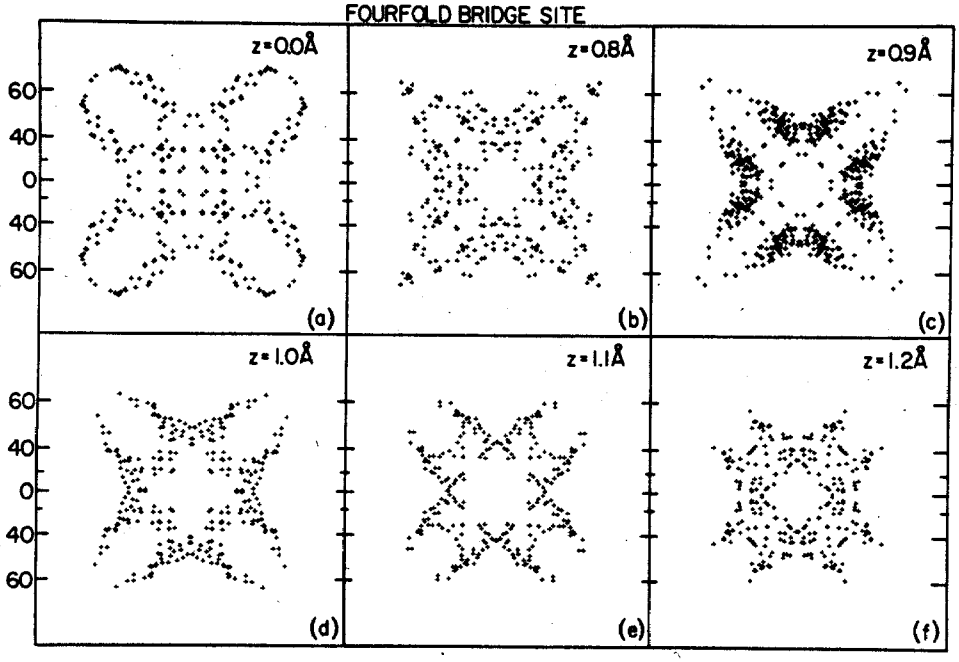


FIG. 2. Angular distributions of oxygen atoms ejected from a fourfold bridge bonded site. The numbers on the ordinate refer to the polar deflection angle given in degrees. All distributions have been symmetrized. Only the oxygen atoms with between 10 and 20 eV of kinetic energy are shown. Heights above the surface of $z = 0.0$, 0.8, 0.9, 1.0, 1.1, and 1.2 Å are shown.

is displayed most compactly by plotting each atom's ultimate position on a flat plate collector at a large distance above the surface. Typical distributions are shown in Fig. 2. The radial extent of a point is proportional to $\tan\theta$, while the azimuthal direction $\phi$ is aligned in the same manner as in Fig. 1. Since the $Ar^+$ ion impacts in a reduced zone instead of the entire surface, the appropriate symmetry operations must be applied to the results to obtain distributions that are comparable to experiment. For example, in the fourfold bridge and atop cases there are four mirror planes and a $C_4$ axis. For the twofold bridge site there are only two mirror planes and a $C_2$ axis; however, experimentally there would probably be two domains rotated by 90°. Thus, we have used the same symmetry operations for all adsorbate positions.

The angular distributions are sensitive to the precise energy range of ejected atoms which are detected. Upon examining various energy ranges, we have arbitrarily chosen to display and discuss only those distributions of particles which have between 10 and 20 eV of kinetic energy. All energy ranges, however, contain information and, when comparisons to experiment are eventually made, *all* particles must be accounted for.

### A. Fourfold bridge site

Examining first the angular distributions of oxygen atoms that were originally in fourfold bridge sites, the patterns for heights of $z = 0.0$, 0.8, 0.9, 1.0, 1.1, and 1.2 Å are shown in Fig. 2. Most of these heights are near the proposed structure as determined from LEED studies,[11] while 0.0 Å approximately corresponds to the oxide structure that is formed when high doses of oxygen are adsorbed.[21] These patterns have several common features. First, the outer envelope encompassing the points is oriented in the $\phi = 45°$ directions. The most intense region, however, is at $\phi \approx 25°$. In addition, there is virtually no ejection normal to the surface, except for the case where the oxygen atoms originate in the surface plane (Fig. 2).

To understand the overall patterns, the detailed motion of the atoms must be considered. By analyzing the results from individual ion impacts, one finds that the total angular distribution is a composite of the distributions of individual atoms. Each contributing atom generally ejects from a set of impact points which are localized in the impact zone. It has a characteristic mechanism of ejection and the distribution of scattering angles from these impact points is fairly localized. The variation in the total angular distribution has two causes. First, the individual atoms which contribute to the total pattern change as the height is varied. For heights between 0.0 and 0.4 Å the atoms labeled O1 and O3 in Fig. 1(a) contribute to the total angular distribution of particles with between 10 and 20 eV of kinetic energy. As the height increases to 0.5–0.8 Å, atoms O2, O4, O5, and O6 are the major contributors, while at heights above 0.9 Å, the pattern is due mainly to O6 with some contribution from O2. The second cause of the variation is that the pattern of an individual atom changes with height. This last cause will be discussed further in the following paragraph.

The ejection of O6, the major contributor to the patterns at heights above 0.9 Å, is controlled by both its bonding site and the height above the surface. In the ejection process, first the $Ar^+$ ion pushes the nickel Ni1 down and in the horizontal direction given by the arrow in Fig. 1(a). Then Ni1 pushes up on Ni2, which subsequently strikes and ejects oxygen O6 in the direction shown by the arrow in Fig. 1(a). Depending on the height of O6, it may also interact with Ni3 or Ni4 as it ejects. The final azimuthal direction of ejection of O6 is controlled by both the initial collision with Ni2 and any possible final channeling by Ni3 or Ni4. Shown in

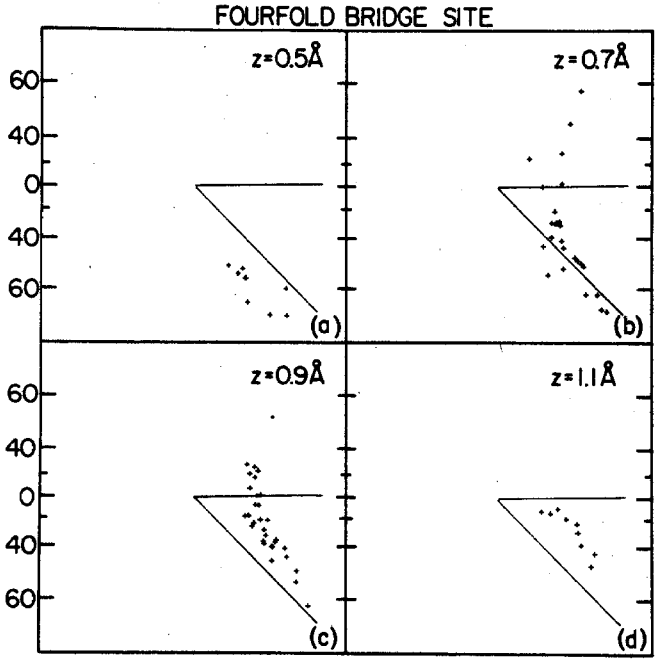


FIG. 3. Unsymmetrized angular distributions of an oxygen atom versus height (see the text). Only oxygen atoms with between 10 and 20 eV of kinetic energy are shown.

Fig. 3 are the unsymmetrized angular distributions of the ejection of O6 at four heights. At the low height of 0.5 Å, O6 collides with Ni4. As the height increases, the interaction with Ni4 decreases; thus, the patterns in Fig. 3 show a counterclockwise rotation with increasing height. In addition, the polar angles tend to get smaller as the height increases. The process is complicated by the fact that the $Ar^+$ ion hits the target oxygen atom O2 before it hits Ni1. Thus, the angle and energy with which Ni2 strikes O6 is also dependent on the oxygen height.

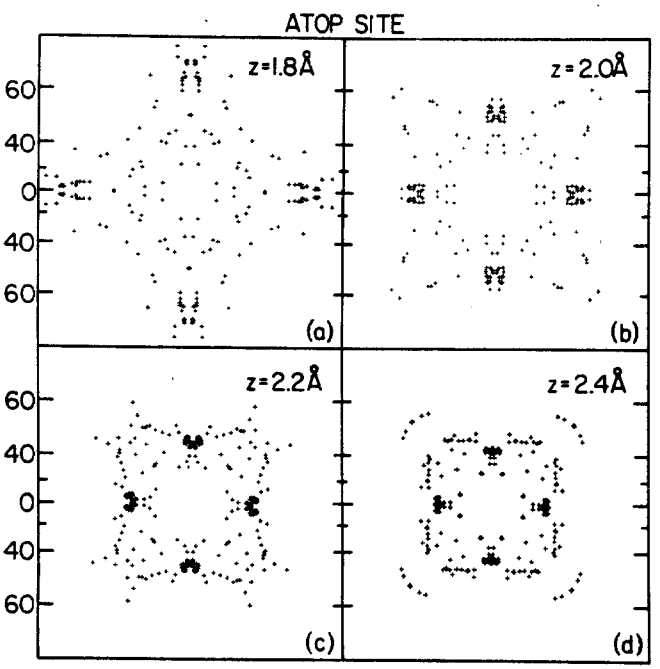


FIG. 4. Angular distributions of oxygen atoms ejected from an atop bonded site. All distributions have been symmetrized. Only the oxygen atoms with between 10 and 20 eV of kinetic energy are shown. Heights above the surface of $z = 1.8$, 2.0, 2.2, and 2.4 Å are shown.

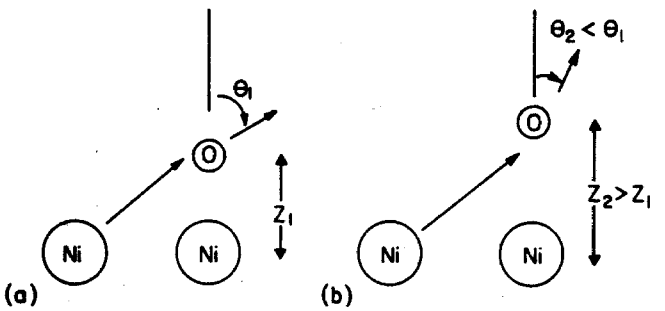


FIG. 5. Mechanisms of ejection of an oxygen atom versus height (see the text).

The target oxygen atom O2 is ejected by the $Ar^+$ ion striking it, forcing O2 to reflect off a neighboring nickel atom and thus ejecting. Oxygen atom O2 tends to eject with more kinetic energy than O6, and the ejection angles are not as well focused as the angles of O6.

### B. Atop site

The angular distributions for ejected oxygen atoms from an atop site are shown in Fig. 4 for heights of 1.8, 2.0, 2.2, and 2.4 Å. The ejection of atoms O7 and O8 of Fig. 1(b) contribute the majority of the pattern with atom O8 giving rise to the distinctive intense region in the $\phi = 0°$ directions. This ejection direction is the same as for the substrate.[7,8,12] The mechanism is easily explained and quite dramatically shows the effect of geometry on the ejection angles of the particles. The neighboring Ni atom [shaded in Fig. 1(b)] is often found to eject with high energy in the $\phi = 0°$ direction. Its direction of ejection is strongly controlled by the surface structure. As this nickel starts to eject, it finds an oxygen atom O8 [Fig. 1(b)] in its way. Since this motion is very nearly coplanar, the oxygen also ejects in the $\phi = 0°$ direction. If the oxygen height is low [Fig. 5(a)], the nickel tends to move "above" it, causing the oxygen to eject with a large or grazing polar angle $\theta_1$. As the oxygen height increases [Fig. 5(b)], the nickel collides "beneath" it and ejects the oxygen atom with a smaller polar angle $\theta_2$. The unsymmetrized angular distributions of atom O8 are shown in Fig. 6 for the same heights as the total patterns in Fig. 4. For the lower heights the oxygen atom O8 ejects at a larger polar angle. As the height increases, the polar angle decreases. Note also the high degree of collimation in the $\phi = 0°$ direction.

If the mechanism pictured in Fig. 5 were as simple as it has been drawn, it would be relatively straightforward to derive an analytical expression for the ejection angle $\theta$ versus height $z$. However, before the nickel strikes the oxygen atom, it has undergone a collision with the $Ar^+$ ion and two of the neighboring nickel atoms. Thus, the motion of the nickel atom before it ejects the oxygen atom cannot be directly determined.

These angular distributions of oxygen atoms ejected

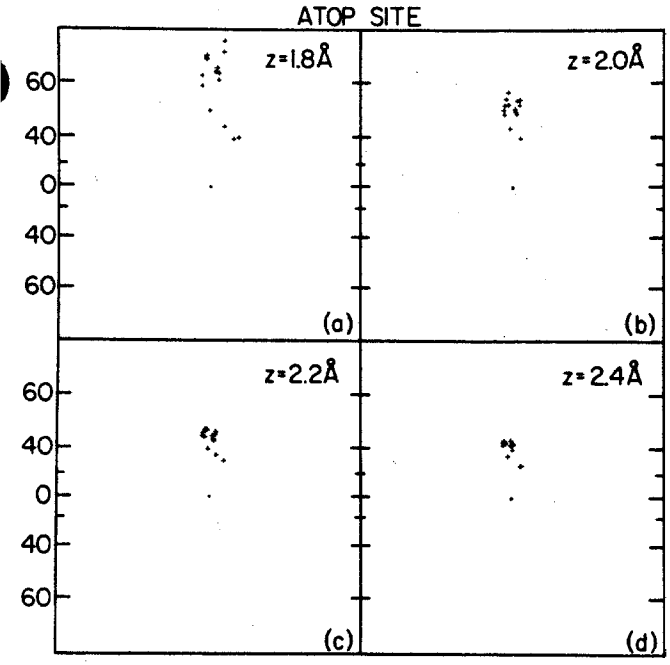


FIG. 6. Unsymmetrized angular distributions of an oxygen atom versus height (see the text). Only oxygen atoms with between 10 and 20 eV of kinetic energy are shown.

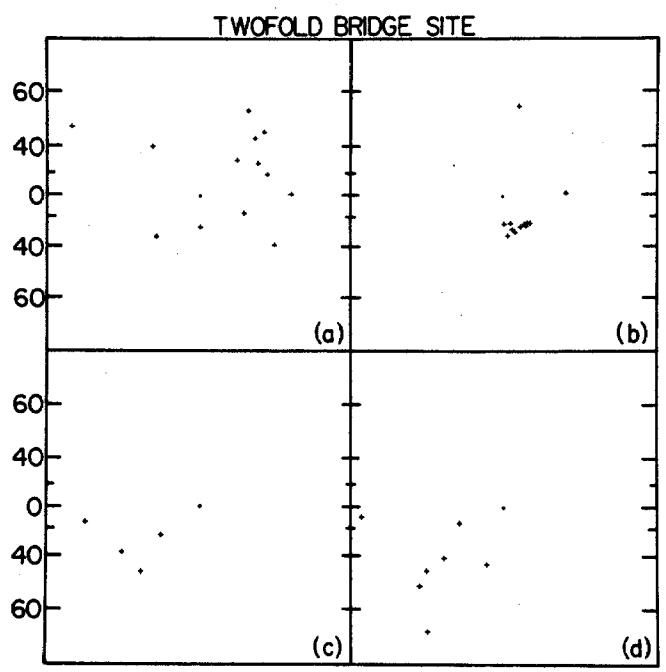


FIG. 8. Unsymmetrized angular distributions of oxygen atoms ejected from a twofold bridge site. The oxygen atoms were originally 1.56 Å above the surface: (a) O11 and O12; (b) O13; (c) O9; (d) O10.

from an atop site are characterized by a region of high intensity in the $\phi = 0°$ direction (Fig. 4). These should be easily distinguished from the distributions arising from atoms originally in a fourfold bridge site (Fig. 2). In addition, the polar angle of the high intensity region is quite sensitive to the adsorbate height.

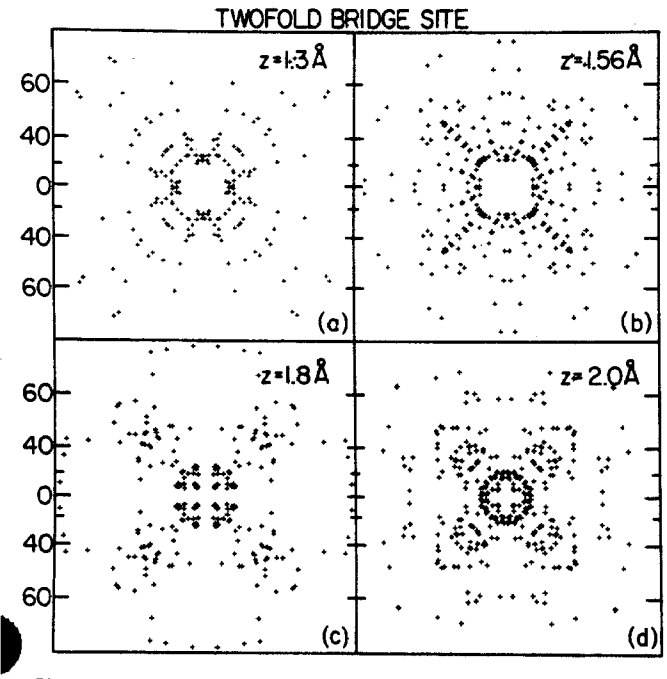


FIG. 7. Angular distributions of oxygen atoms ejected from a twofold bridge bonded site. All distributions have been symmetrized. Only the oxygen atoms with between 10 and 20 eV of kinetic energy are shown. Heights above the surface of $z$ = =1.3, 1.56, 1.8, and 2.0 Å are shown.

### C. Twofold bridge site

The final adsorption position examined is a twofold bridge bonded site. The angular distributions of oxygen atoms with 10 to 20 eV of energy for heights of 1.3, 1.56, 1.8, and 2.0 Å are shown in Fig. 7. In contrast to the previous two sites examined, here no one ejection mechanism dominates the overall pattern. There are five oxygen atoms, labeled O9–O13 in Fig. 1(c), which contribute to the oxygen pattern. Due to the reduced symmetry for the twofold bridge site, the impact zone is larger than for the other two sites, such that there are two target oxygen atoms O11 and O12. As in the fourfold bridge site case, these atoms tend to eject with higher energies and in unfocused directions [Fig. 8(a)].

The ejection of O13 is caused by the contiguous nickel atom Ni5. The ejection direction is almost normal to the surface [Fig. 8(b)]. In neither the fourfold bridge case nor the atop case was there a mechanism that resulted in this type of normal ejection. The ejection of O9 and O10 [Figs. 8(c) and 8(d), respectively] is caused by interactions with oxygen O11 which had been struck by the $Ar^+$ ion.

The angular distributions of oxygen atoms ejected from the twofold bridge sites exhibit several common features. There is a lack of intensity in the $\phi = 0°$ direction which is present for the atop case and to a lesser extent in the fourfold bridge case. There is more intensity in the normal direction than is present in the fourfold bridge case. In addition, the overall angular distributions are more scattered than in the other cases discussed.

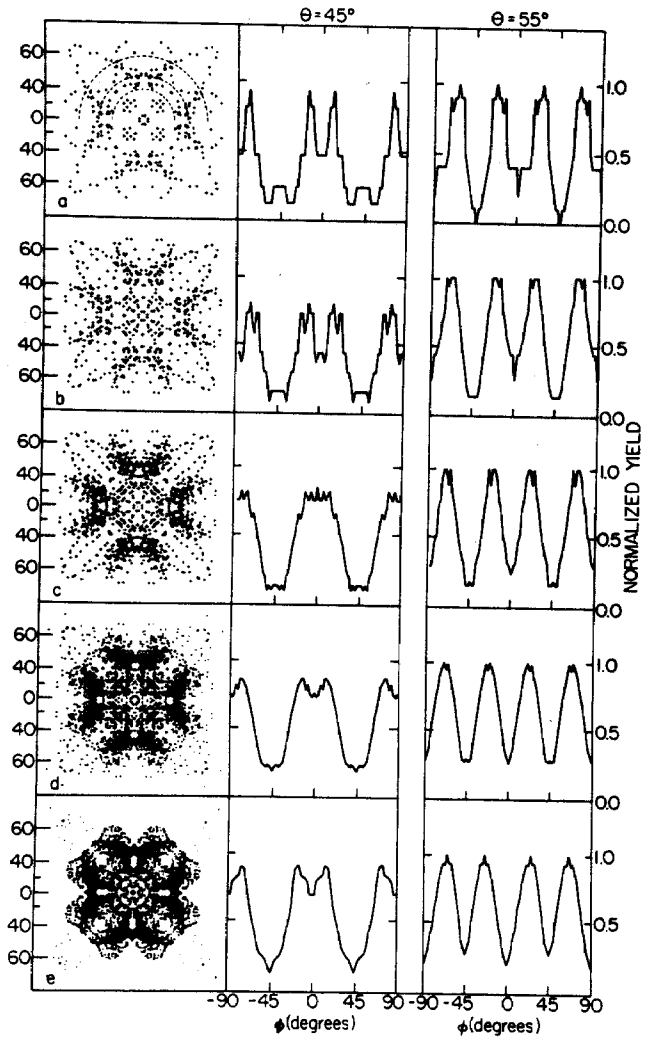


FIG. 9. Convergence of oxygen atom angular distributions versus number of $Ar^+$ ion impacts. Flat plate collector and $\phi$ plots for $\theta = 45° \pm 5°$ and $55° \pm 5°$ are shown. The oxygen atoms were originally in a fourfold bridge site 0.9 Å above the surface. Particles with greater than 10 eV of kinetic energy are shown. Frame (a) has concentric circles drawn at $\theta = 40°$ and $\theta = 50°$ showing which atoms contribute to the $\phi$ plot for $\theta = 45°$ (similarly for the $\theta = 55°$ plot). (a) 55 $Ar^+$ ion impacts; (b) 100 $Ar^+$ ion impacts; (c) 165 $Ar^+$ ion impacts; (d) 300 $Ar^+$ ion impacts; (e) 500 $Ar^+$ ion impacts.

### D. Comparisons with experiment

Although the flat plate collector type plots conveniently display the entire angular distribution, it is difficult to make quantitative comparisons to experimental data with this representation. Another possible way of displaying the calculated angular distributions is for a fixed polar angle $\theta$ to plot the intensity of particles as a function of the azimuthal angle $\phi$. Examples of these azimuthal distributions or $\phi$ plots are shown in Fig. 9 for polar angles of $\theta = 45° \pm 5°$ and $55° \pm 5°$ for oxygen in a fourfold bridge site 0.9 Å above the surface. Here, all the oxygen atoms whose energy is greater than 10 eV are shown. For these distributions the size of the solid angle of collection $\Delta\Omega$, where

$$\Delta\Omega = \sin\theta \Delta\theta \Delta\phi \ ,$$

is held constant. The angle of collection in the polar direction $\Delta\theta$ is also specified and is constant. Thus, we approximate

$$\Delta\phi \simeq \Delta\theta / \sin\theta \ .$$

This is physically reasonable since at $\theta = 0°$ or ejection normal to the surface an azimuthal angle cannot be defined. For $\theta \to 90°$ or grazing angles of ejection, the $\phi$ collection angle is the same as the $\theta$ collection angle. A value of $\Delta\theta = 10°$ is chosen as a reasonable estimate of experimental resolutions.[12]

The experimental angular resolution is approximately convoluted into the calculated $\phi$ plots. The points are spaced quite closely (every 1°–2°) in $\phi$ with the intensity at each point representing the particles with an azimuthal angle in the range $\phi \pm \Delta\phi/2$. This appears to give the most realistic comparison to the experimental results. The results have all had the appropriate symmetry operations applied to them; thus, only the information from $\phi = 0°$ to 45° is unique. A wider angle range is plotted for visual clarity. The intensity is scaled to the maximum intensity of all polar angles.

The angular distributions of the ejected oxygen atoms, represented as flat plate collector displays and as $\phi$ plots, are shown in Fig. 9 as a function of the number of $Ar^+$ ion impacts. For cases (a), (b), (c), and (d), 55, 100, 165, and 300 impact points, respectively, were employed where the points in (a) are a subset of the ones in (b), etc. There were 500 distinct impact points utilized in Fig. 9(e). The basic features of the angular distributions are apparent with only 55–100 $Ar^+$ ion impacts. In the $\theta = 55°$ azimuthal distributions, there is a peak at $\phi \simeq 25°$, as discussed in Sec. III A, and no apparent fine structure. More ion impacts are needed, however, to resolve the fine structure in the $\theta = 45°$ azimuthal distribution. There is a sizable dip at $\phi = 0°$ in case (a), which disappears in case (c) (165 ion impacts), but reforms to a lesser extent in cases (d) and (e) (300 and 500 ion impacts, respectively). Examining the flat plate collector display, in conjunction with the $\phi$ plots, shows a region at $\phi = 0°$ with $\theta$ between 40° and 50° with no intensity. The detailed distributions such as $\phi$ plots and more global ones such as the flat plate collector provide different prospectives for ascertaining the significance of the fine structure in the angular distributions.

An effect of energy selection of the ejected particles can be seen by comparing Figs. 2(c) and 9(b). They are from the same set of data, except that particles with 10–20 eV are displayed in Fig. 2(c), while all particles with greater than 10 eV of kinetic energy are displayed in Fig. 9(b). As discussed in Sec. III A, the additional scattered points at the higher energies arise primarily from the ejection of the target oxygen atom O2.

## IV. SUMMARY AND CONCLUSIONS

The angular distributions of oxygen atoms ejected during the ion bombardment of a $c(2\times2)$ overlayer of oxygen on Ni (001) show a strong sensitivity to adsorption site and the height of the adsorbate above the sur-

face. Under optimal conditions one should be able to use these angular distributions to determine experimentally the bonding site of an adsorbate and its original height above the surface. Unfortunately, there are several factors which will add confusion to the interpretation of the experimental angular distributions. First, the interaction potentials are *not* known. As will be shown in a future study,[14] the choice of potential does influence the angles of ejection. The characteristics of the angular distributions associated with the bonding site are less affected by changes in the interaction potential than the features associated with the height of the adsorbate. A second consideration is that the calculations have been performed for an initially rigid crystal while the experimental spectra may possibly show some thermal effects. This can be incorporated into the theoretical model, but with considerably more effort. Finally, there is the problem that presently the experimental angular distributions that are measured will be those of ions while the calculated ones are for neutral atoms. Initial experiments indicate that it is possible to make comparisons of the neutral and ion motions by adjusting the calculated neutral momenta for the image force that the ion experiences as it leaves the solid.[22]

## ACKNOWLEDGMENTS

We would like to gratefully acknowledge discussions with N. Winograd and S. Holland. In addition, one of us (BJG) acknowledges support from the Camille and Henry Dreyfus Foundation for a grant for Newly Appointed Young Faculty, the Alfred P. Sloan Foundation for a Research Fellowship, the Research Corporation for a Cottrell grant, and the Pennsylvania State University for a Research Initiation grant. The work was also supported in part by a grant from the National Science Foundation (Grant No. CHE-8022524). We are also grateful to K. Foley for critically reading the manuscript.

[1]See, for example, M. A. van Hove and S. Y. Tong, *Surface Crystallography by LEED*, Springer Series in Chemical Physics (Springer, Berlin, 1979), Vol. 2.
[2]See, for example, T. E. Madey and J. T. Yates, Surf. Sci. **63**, 203 (1977).
[3]See, for example, H. Ibach, H. Hopster, and B. Sexton, Appl. Surf. Sci. **1**, 1 (1977).
[4]E. Taglauer and W. Heiland, Appl. Phys. **9**, 261 (1976).
[5]P. H. Citrin, D. Eisenberger, and R. C. Hewitt, Phys. Rev. Lett. **41**, 309 (1978).
[6]S. P. Holland, B. J. Garrison, and N. Winograd, Phys. Rev. Lett. **43**, 220 (1979).
[7]N. Winograd, B. J. Garrison, and D. E. Harrison, Jr., Phys. Rev. Lett. **41**, 1120 (1978).
[8]S. P. Holland, B. J. Garrison, and N. Winograd, Phys. Rev. Lett. **44**, 756 (1980).
[9]Observed from a Ni(001) crystal with an overlayer of sulfur. S. P. Holland and N. Winograd (unpublished results).
[10]N. Winograd, S. P. Holland, K. E. Foley, and R. A. Gibbs, Vide **201**, 427 (1980).
[11](a) M. van Hove and S. Y. Tong, J. Vac. Sci. Technol. **12**, 230 (1975); (b) J. E. Demuth, D. W. Jepsen, and P. M. Marcus, Phys. Rev. Lett. **31**, 540 (1973).
[12]R. A. Gibbs, N. Winograd, Rev. Sci. Instrum. (submitted).
[13]V. E. Yurasova, A. A. Sysoev, G. A. Samsonov, V. M. Burkhanov, L. N. Nevzovova,and L. B. Shelyakin, Radiat. Eff. **20**, 89 (1973).
[14]S. Kapur and B. J. Garrison, Surf. Sci. Lett. (in press).
[15]D. E. Harrison, Jr., P. W. Kelly, B. J. Garrison, and N. Winograd, Surf. Sci. **76**, 311 (1978).
[16]B. J. Garrison, N. Winograd, and D. E. Harrison, Jr., Phys. Rev. B **18**, 6000 (1978).
[17]N. Winograd, K. E. Foley, B. J. Garrison, and D. E. Harrison, Jr., Phys. Lett. A **73**, 253 (1979).
[18]N. Winograd, B. J. Garrison, and D. E. Harrison, Jr., J. Chem. Phys. **73**, 3473 (1980).
[19]D. E. Harrison, Jr., W. L. Moore, Jr., and H. T. Holcombe, Radiat. Eff. **17**, 167 (1973).
[20]L. A. Girafalco and V. G. Weizer, Phys. Rev. **114**, 687 (1959).
[21]L. G. Peterson, S. Kono, N. F. T. Hall, S. Goldberg, J. T. Lloyd, C. S. Fadley, and J. Pendry, Mater. Sci. Eng. **42**, 111 (1980).
[22]R. A. Gibbs, S. P. Holland, K. E. Foley, B. J. Garrison, and N. Winograd (manuscript in preparation).